

# Photocontrolled Light-Harvesting Supramolecular Assembly Based on Aggregation-Induced Excimer Emission

Jing-Jing Li, Heng-Yi Zhang,\* Guoxing Liu, Xianyin Dai, Lei Chen, and Yu Liu\*

Photocontrolled light-harvesting supramolecular assembly with aggregation-induced excimer emission is fabricated by polyanionic  $\gamma$ -cyclodextrin (COONa- $\gamma$ CD), pyrene derivative (PYC12), Nile red (NiR), and diarylethene derivative (DAE) in aqueous solution. Benefiting from the COONa- $\gamma$ CD-induced aggregation of PYC12, the fluorescence can be modulated from monomeric state to assembled state with a large red-shift around 100 nm, which exhibits aggregation-induced excimer emission enhancement and makes PYC12 a remarkable energy donor. Subsequently, NiR can function as energy acceptor loaded into PYC12/COONa- $\gamma$ CD supramolecular assembly, and highly efficient energy transfer process occurs from PYC12/COONa- $\gamma$ CD to NiR, with energy transfer efficiency up to 83% at donor/acceptor ratio of 160:1. Moreover, multicolor tunable emission can be achieved simply by tuning the molar ratios of donor and acceptor, notably including white-light emission. Interestingly, loading photoresponsive energy acceptor DAE into PYC12/COONa- $\gamma$ CD/NiR assembly endows the light-harvesting system with excellent photocontrolled energy transfer, and this process can be efficiently regulated upon distinct light irradiation.

Light harvesting is one of the most important parts in natural photosynthesis in which a large number of antenna chromophores harvest light energy and the excitation energy subsequently transfers to the reaction center, where light energy turns into chemical energy.<sup>[1]</sup> Mimicking light-harvesting system provides a theoretical basis to understanding the process of photosynthesis, and leads to the potential applications in solar cells,<sup>[2]</sup> photoelectric materials,<sup>[3]</sup> photocatalysis,<sup>[4]</sup> photodynamic therapy,<sup>[5]</sup> biological imaging,<sup>[6]</sup> and biosensor.<sup>[7]</sup> Inspired by nature, considerable efforts have been devoted to mimic natural light-harvesting process with satisfactory energy transfer efficiency.<sup>[8]</sup> Toward this goal, some essential points should be taken into account: the donors should require orderly tight spatial organization, and avoid aggregation-caused quenching (ACQ) effect due to compact arrangement; the energy donor and energy acceptor must have a good spectral overlap and suitable distance in order to minimize energy loss; and the donor/acceptor ratio

should be relatively high.<sup>[9]</sup> Considering the advantages of host-guest interaction, supramolecular assembly with macrocycle has turned out to be a useful approach to develop aqueous light-harvesting systems.<sup>[10]</sup> For example, Tang and co-workers reported an efficient light-harvesting system with ultrahigh antenna effect based on aggregation-induced enhanced emission (AEE) conjugated polymeric supramolecular network.<sup>[11]</sup> Anderson and co-workers synthesized a complex comprising a cyanine dye rotaxane and a porphyrin nanoring as a model light-harvesting system.<sup>[12]</sup> Wang and coworkers fabricated highly efficient artificial light-harvesting systems based on supramolecular self-assembly.<sup>[4a,13]</sup> Our group also developed aqueous light-harvesting systems with efficient energy transfer efficiency.<sup>[14]</sup>

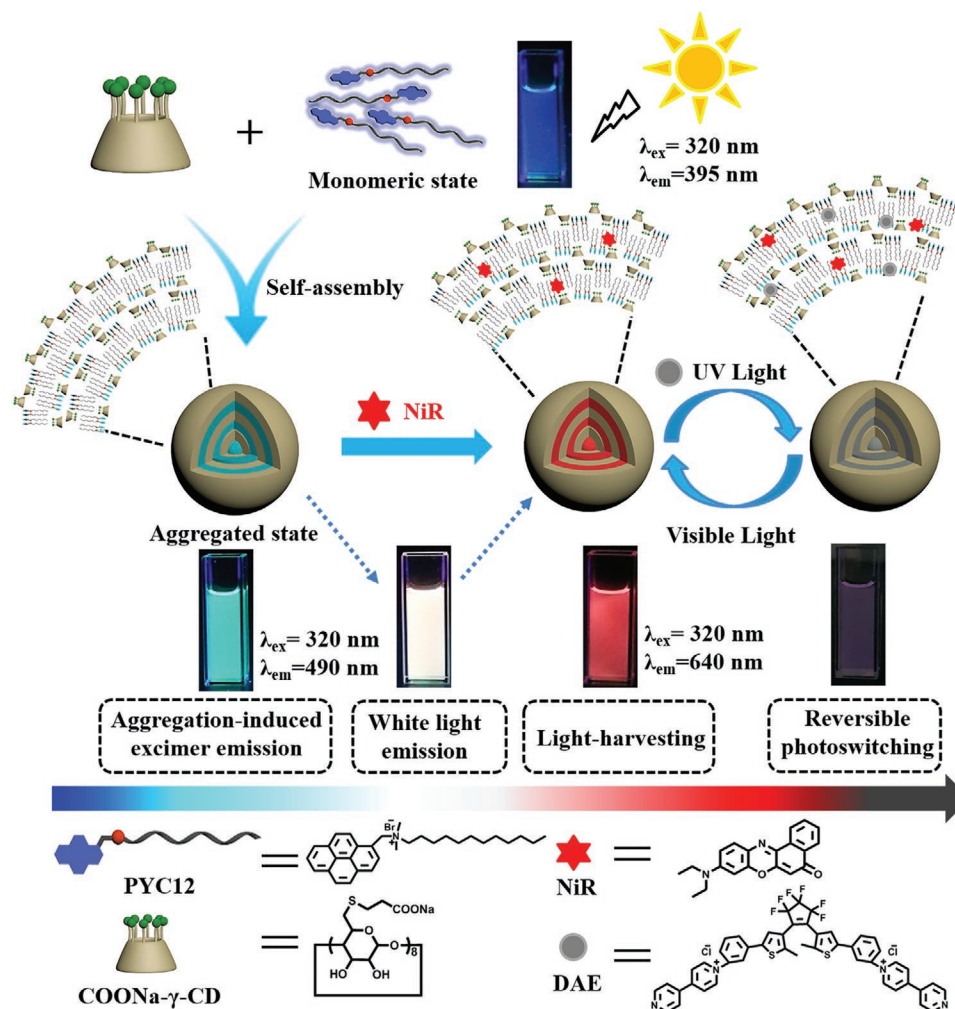
Antenna chromophores with distinct fluorescence property play a significant role in light-harvesting systems.

In this regard, some people have paid increasing attention to improving the photophysical properties of optical materials to achieve high quantum yield, strong emission, and broad color emission.<sup>[15]</sup> Traditional luminophores have suffered from the undesired ACQ effect in aggregated state because of intermolecular compact  $\pi$ - $\pi$  stacking, which severely limits their further applications in aqueous solution. On the contrary, organic fluorogens with aggregation-induced emission are highly emissive in aggregated state, which exhibits remarkable advantages to construct light-harvesting systems.<sup>[16]</sup> However, fluorophores with stacked-induced excimer emission characteristics typically provide a broad spectrum with the maximum red-shifted around 100 nm in aggregated state compared to monomer emission,<sup>[17]</sup> which overcomes the ACQ effect and is not restricted to the UV or blue regions in water. Therefore, constructing light-harvesting systems by tuning a single fluorophore's photoluminescence from monomer emission in monomeric state to excimer emission in aggregated state was rarely reported to our knowledge. Herein, we fabricated novel photo-controlled light-harvesting system based on the supramolecular assembly of polyanionic  $\gamma$ -cyclodextrin (COONa- $\gamma$ CD), pyrene derivative (PYC12), Nile red (NiR), and diarylethene derivative (DAE) in aqueous solution (**Scheme 1**). PYC12 displays intense fluorescence emission at 375 and 395 nm in isolated or monomeric state, whereas they produce strong red-shift excimer emission at 490 nm in the aggregated state. COONa- $\gamma$ CD could induce efficient aggregation into well-ordered PYC12/COONa- $\gamma$ CD

Dr. J.-J. Li, Dr. H.-Y. Zhang, Dr. G. Liu, Dr. X. Dai, Dr. L. Chen, Prof. Y. Liu  
Department of Chemistry  
State Key Laboratory of Elemento-Organic Chemistry  
Nankai University  
Tianjin 300071, P. R. China  
E-mail: hyzhang@nankai.edu.cn; yuliu@nankai.edu.cn

 The ORCID identification number(s) for the author(s) of this article can be found under <https://doi.org/10.1002/adom.202001702>.

DOI: 10.1002/adom.202001702



**Scheme 1.** Schematic illustration of photocontrolled supramolecular light-harvesting system.

supramolecular assembly, improving the aggregation-induced excimer emission properties of PYC12 and enabling PYC12 to act as a remarkable energy donor. Subsequently, NiR acting as energy acceptor could be loaded into the hydrophobic interior of PYC12/COONa- $\gamma$ -CD assembly. As a result, a highly efficient energy transfer process occurs from PYC12/COONa- $\gamma$ -CD assembly to the loaded NiR, and we achieved a broad-spectrum multicolor photoluminescence by tuning the donor/acceptor ratio, notably including white-light emission. Furthermore, a photoresponsive energy acceptor DAE was encapsulated into the PYC12/COONa- $\gamma$ -CD/NiR light-harvesting assembly; photocontrolled energy transfer between quenching and emission was achieved due to the reversible cyclization/cycloreversion of DAE upon irradiation with UV or visible light.

Pyrene is a tetracyclic aromatic hydrocarbon with strong and stable fluorescence emission. The pyrene fluorophore displays a free monomer state in dilute solution, whereas they can produce red-shifted excimer emission when stacked into a dimer state.<sup>[18]</sup> Considering the distinct excimer emission of pyrene moiety, a new PYC12 with a quaternary ammonium salt and hydrophobic alkyl chain was conveniently synthesized (Figures S1–S3, Supporting Information). Figure S4a, Supporting Information,

exhibits the UV–vis absorbance spectrum of different concentration of PYC12. As evident from Figure S4b, Supporting Information, PYC12 displays deep-blue monomeric emission at 375 and 395 nm in dilute solution, while a broad emission peak at 490 nm with a large Stokes shift appeared by the increased concentration of PYC12, which is consistent with previous reports in the literature.<sup>[18a]</sup> The new emission at 490 nm was attributed to the excimer emission of the stacked pyrene. However, with the increase of concentration, the emission intensity of PYC12 at 490 nm decreased due to the ACQ.

Taking advantage of the distinct excimer emission features of PYC12, we considered whether COONa- $\gamma$ -CD could induce the aggregation of PYC12 to generate excimer emission in dilute solution. As shown in Figure 1b, the addition of COONa- $\gamma$ -CD lead to the monomeric emission of PYC12 at 375 and 395 nm significantly decreased, along with the emergence of excimer emission peaks at 490 nm. The fluorescence intensity at 490 nm was increased by gradually adding COONa- $\gamma$ -CD to PYC12 solution, Stokes shift reached 170 nm. CIE chromaticity diagram displayed a color variation from deep-blue to cyan with the addition of COONa- $\gamma$ -CD (Figure 1c). The phenomenon of aggregation-induced excimer emission enhancement

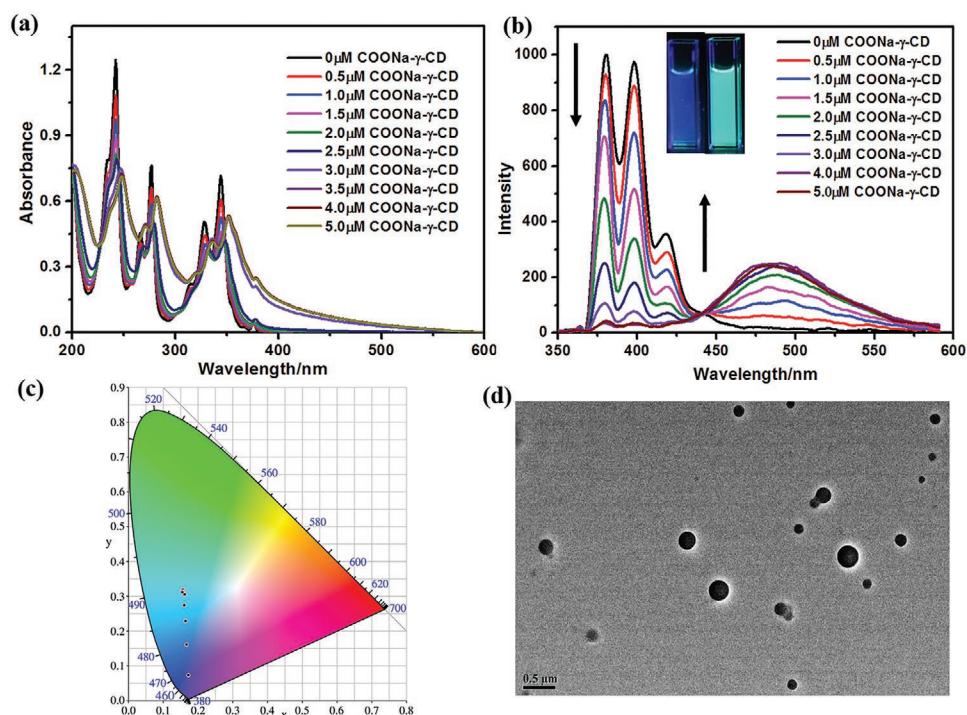


**Figure 1.** a) Absorbance spectra and b) fluorescence emission spectra of PYC12 with the addition of COONa- $\gamma$ -CD. Inset: photographs of PYC12 (left) and PYC12/COONa- $\gamma$ -CD (right) under 365 nm. c) The CIE chromaticity diagram showing the photoluminescence color changes of PYC12 with the addition of COONa- $\gamma$ -CD. d) TEM image of PYC12/COONa- $\gamma$ -CD assembly ( $\lambda_{\text{ex}} = 320 \text{ nm}$ , PYC12 =  $20 \times 10^{-6} \text{ M}$ , COONa- $\gamma$ -CD =  $3 \times 10^{-6} \text{ M}$ ).

was readily observed by naked eyes. The increased excimer emission was attributed to formation of PYC12 aggregates induced by highly anionic COONa- $\gamma$ -CD. Then, the addition of an excess amount of COONa- $\gamma$ -CD led to the formation of a simple inclusion complex accompanied by the disassembly of the aggregates, resulting in the excimer emission at 490 nm decreased, along with an increase of monomer emission (Figure S7b, Supporting Information). Meanwhile, UV-vis titration experiment was performed by adding COONa- $\gamma$ -CD into PYC12 solution (Figure 1a). By gradually adding COONa- $\gamma$ -CD to the PYC12 solution at fixed concentration of  $20 \times 10^{-6} \text{ M}$ , the absorbance spectra exhibited drastically broadening and redshift at the  $3 \times 10^{-6} \text{ M}$  COONa- $\gamma$ -CD (Figure S8a, Supporting Information), indicating the aggregation of PYC12 to form large supramolecular assembly. Subsequently, with the further addition of COONa- $\gamma$ -CD (Figure S8b, Supporting Information), the absorbance spectra exhibited obvious blue-shift and decreased, indicating the large supramolecular assembly disaggregated. Subsequently, under the same experimental conditions, we added  $\alpha$ -cyclodextrin ( $\alpha$ -CD),  $\beta$ -cyclodextrin ( $\beta$ -CD), or  $\gamma$ -cyclodextrin ( $\gamma$ -CD) into PYC12 solution, and the fluorescence emission of PYC12 was nearly unchanged (Figure S11, Supporting Information). Moreover, its absorption and fluorescence emission did not change even by adding 5 equiv. cyclodextrin to PYC12 solution (Figure S12, Supporting Information), indicating that electrostatic interaction plays an important role in inducing the aggregation of PYC12 to form excimer emission, rather than the inclusion of the cavity. In order to prove the importance of electrostatic interaction in inducing the aggregation of PYC12, we choose different macrocyclic

hosts with negative charge as reference, both COONa- $\beta$ -CD and SC4A can induce the aggregation of PYC12 and produce enhanced excimer emission (Figure S6, Supporting Information). Then we investigated the  $^1\text{H}$  NMR spectrum (Figure S9, Supporting Information) of PYC12 with COONa- $\gamma$ -CD. As can be seen from Figure S9, Supporting Information, almost all proton peaks of free PYC12 broaden, suggesting there exist the intermolecular aggregation between PYC12 molecules. With the addition of COONa- $\gamma$ -CD (0.25 equiv.), the proton signals of pyrene exhibited further drastically broaden because COONa- $\gamma$ -CD induced the aggregation of PYC12 by the electrostatic interactions, making them unidentifiable. The results indicated that electrostatic interactions play the leading role between PYC12 and COONa- $\gamma$ -CD at low COONa- $\gamma$ -CD concentration. Upon the further addition of COONa- $\gamma$ -CD (0.5, 1, 1.5, 2.0 equiv.), the proton signals of pyrene reappeared accompanying with obvious low-field shift because of the disassembly to the formation of simple inclusion complex when the amount of COONa- $\gamma$ -CD was excess. Then the rotating frame overhauser effect spectroscopy (ROESY) spectrum (Figure S10, Supporting Information) showed a clear correlation between pyrene moiety of PYC12 and COONa- $\gamma$ -CD, indicating the host-guest inclusion occurs when the amount of COONa- $\gamma$ -CD was excess. In addition, we selected the model molecule 1-pyrene methylamine hydrochloride (PMH) as a control experiment. Fluorescence titration and UV-vis titration spectrum indicate that it did not stack into aggregated state to generate 490 nm excimer emission (Figure S13a,b, Supporting Information). Maybe it forms a simple inclusion complex and the stoichiometry of the complex and association constant was investigated

by using UV–vis spectroscopy, the Job's plot showed the 1:1 binding stoichiometry and the association constant was  $7.3 \times 10^5 \text{ M}^{-1}$  between 1-pyrene methylamine hydrochloride and COONa- $\gamma$ CD (Figure S13c,d, Supporting Information). The results indicated that hydrophobic alkyl chain also plays an important role in inducing excimer emission in this supramolecular assembly. Based on the above experimental results, we found that COONa- $\gamma$ CD could induce the aggregation of PYC12 by the electrostatic interaction to modulate the fluorescence from monomer emission at 395 nm to excimer emission at 490 nm, accompanying with a red shift of about 100 nm.

The induced aggregation behavior and morphology of PYC12/COONa- $\gamma$ CD assembly were further investigated through optical transmittance, transmission electron microscopy (TEM), Tyndall effect, dynamic light scattering (DLS), and zeta potential. The critical aggregation concentrations (CAC) of PYC12 at 25 °C were measured as  $0.6 \times 10^{-3} \text{ M}$  (Figure S5, Supporting Information). Upon the addition of COONa- $\gamma$ CD, the optical transmittance of PYC12 at 450 nm decreased because of the formation of large supramolecular assembly, and an inflection point at  $12 \times 10^{-6} \text{ M}$  was observed (Figure S14a,b, Supporting Information). Therefore, an aggregation induced CAC value of PYC12 was  $12 \times 10^{-6} \text{ M}$  in the presence of COONa- $\gamma$ CD. Moreover, the preferable mixing ratio between COONa- $\gamma$ CD and PYC12 was also investigated. By gradually adding COONa- $\gamma$ CD to the PYC12 solution at fixed concentration of  $20 \times 10^{-6} \text{ M}$ , the optical transmittance at 450 nm decreased rapidly and then gradually increased thereafter to a quasi-plateau, and an inflection point at  $3 \times 10^{-6} \text{ M}$  was observed (Figure S14c,d, Supporting Information), which indicated the best mixing concentration was  $20 \times 10^{-6} \text{ M}$  PYC12 and  $3 \times 10^{-6} \text{ M}$  COONa- $\gamma$ CD. Moreover, There is no obvious change in the optical transmittance of PYC12/COONa- $\gamma$ CD assembly within 6 h in aqueous solution (Figure S17, Supporting Information), indicating the good stability of obtained nanoparticles. Subsequently, a simple mixing of COONa- $\gamma$ CD and PYC12 exhibited an obvious Tyndall effect in aqueous solution (Figure S15f, Supporting Information), indicating the formation of large supramolecular assembly. However, only PYC12 did not exhibit Tyndall effect (Figure S15e, Supporting Information), revealing that PYC12 did not form large self-aggregates under the same conditions. Both TEM (Figure S15a, Supporting Information) and SEM (Figure S16, Supporting Information) images of PYC12/COONa- $\gamma$ CD supramolecular assembly displayed several spherical nanoparticles with a diameter of  $\approx 100\text{--}300 \text{ nm}$ . The DLS results illustrated the formation of supramolecular assembly with an average diameter of  $\approx 387 \text{ nm}$ , accompanied by a narrow size distribution (Figure S15b, Supporting Information). Moreover, the zeta potential of PYC12/COONa- $\gamma$ CD was measured as  $-9.24 \text{ mV}$  (Figure S15g, Supporting Information), suggesting that the surfaces of the supramolecular nanoparticles were negatively charged.

Excellent photoluminescence properties and orderly tight spatial organization are essential criteria for designing supramolecular light-harvesting system, which could facilitate excitation energy transfer and minimize energy loss from donor to acceptor. In the present case, COONa- $\gamma$ CD could induce the aggregation of PYC12 to form orderly tight stacking supramolecular assembly by the electrostatic interaction,  $\pi$ - $\pi$  stacking,

and hydrophobic interaction, which induced distinct excimer emission properties. Thus, PYC12/COONa- $\gamma$ CD supramolecular assembly as energy donor should be potential promising to fabricate artificial light-harvesting systems with high energy transfer efficiency in aqueous solution. Organic dye could be loaded into the interior hydrophobic environment of supramolecular assembly to avoid self-quenching and shorten the distance with donor chromophores to achieve effective Förster resonance energy transfer (FRET) process. Subsequently, hydrophobic fluorescent dye NiR or Eosin Y (EY) as energy acceptor was loaded into the PYC12/COONa- $\gamma$ CD supramolecular assembly because the emission of PYC12/COONa- $\gamma$ CD overlaps well with the absorption of the NiR or EY (Figure 2a,c), which promise the feasibility of energy transfer. As shown in Figure 2b, with the gradual addition of NiR to the PYC12/COONa- $\gamma$ CD assembly, the fluorescence intensity of PYC12/COONa- $\gamma$ CD assembly (donor) at 490 nm decreased, while the fluorescence emission of NiR (acceptor) at 640 nm increased when excited at 320 nm, and an obvious antenna effect occurred even in the donor/acceptor ratio up to 2000:1. In the absence of PYC12/COONa- $\gamma$ CD assembly, the fluorescence of free NiR was negligible under the same conditions (Figure S20, Supporting Information). In addition, there was no obvious change of fluorescence intensity with the addition of NiR to PYC12 solution (Figure S21, Supporting Information), indicating that PYC12/COONa- $\gamma$ CD assembly contributes to the amplified NiR emission directly. These results both suggested that NiR was loaded into the interior of PYC12/COONa- $\gamma$ CD assembly, the energy was successfully transferred from donor PYC12/COONa- $\gamma$ CD to acceptor NiR in aqueous solution despite the low concentrations of them (PYC12 =  $20 \times 10^{-6} \text{ M}$  and NiR =  $0.125 \times 10^{-6} \text{ M}$ ), and an efficient aqueous light-harvesting system was obtained. To quantitatively evaluate the ability of light-harvesting system, we calculated the energy transfer efficiency and antenna effect. Consequently, the energy transfer efficiency was calculated as 83% (Figure S18, Supporting Information), and antenna effect was calculated as 15.8 (Figure S19, Supporting Information) at a donor/acceptor ratio of 160:1. Furthermore, EY as energy acceptor was also used to construct another light-harvesting system. As shown in Figure 2d, efficient energy transfer from PYC12/COONa- $\gamma$ CD assembly to EY was also realized with the addition of EY. Similarly, free EY without PYC12/COONa- $\gamma$ CD assembly barely fluoresced (Figure S24, Supporting Information), and there was no obvious change of fluorescence intensity with the addition of EY to PYC12 solution under the same condition (Figure S25, Supporting Information). According to the fluorescence titration spectrum, the energy transfer efficiency was calculated as 80.2% (Figure S22, Supporting Information), and antenna effect was calculated as 25.4 (Figure S23, Supporting Information) at a donor/acceptor ratio of 250:1. Subsequently, the excited state lifetimes of PYC12/COONa- $\gamma$ CD assembly was significantly decreased upon the addition of NiR or EY, further validated the energy transfer process. It should be mentioned that there are no appreciable photobleaching was observed for the present systems (Figure S26, Supporting Information). Fluorescence lifetime experiments exhibited that the decay curve of PYC12 followed a double exponential decay with  $\tau_1 = 26.37 \text{ ns}$  and  $\tau_2 = 126.5 \text{ ns}$  (Figure S27, Supporting

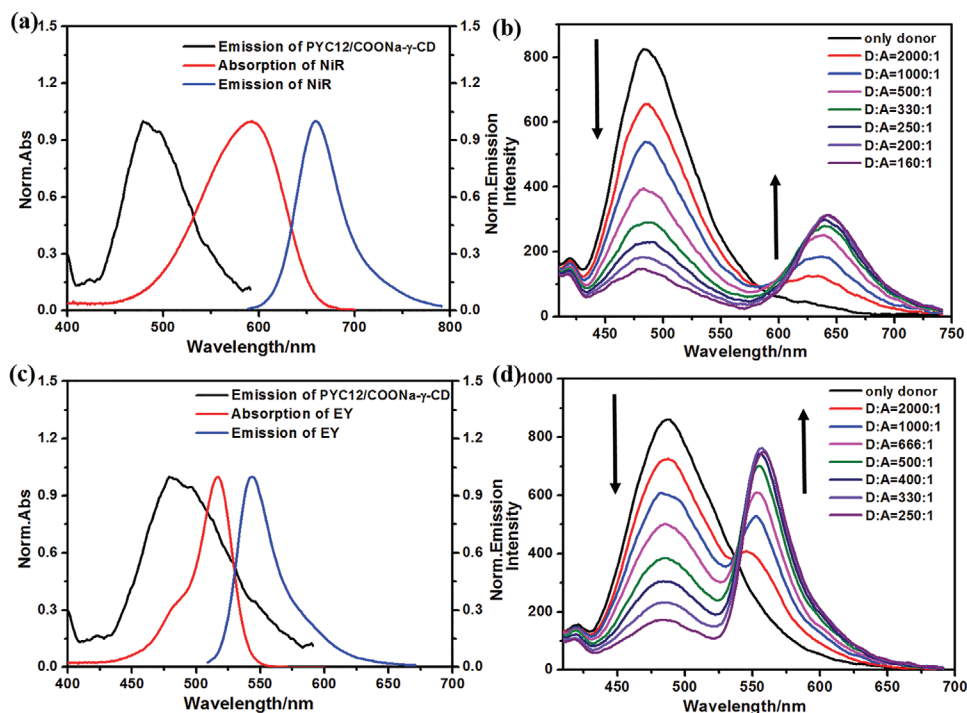


**Figure 2.** a) Normalized emission spectra of PYC12/COONa- $\gamma$ CD, and absorption and emission spectra of NiR. b) Fluorescence spectra of PYC12/COONa- $\gamma$ CD (PYC12 =  $20 \times 10^{-6}$  M, COONa- $\gamma$ CD =  $3 \times 10^{-6}$  M) with different concentration of NiR. The concentrations of NiR were  $0.00 \times 10^{-6}$ ,  $0.01 \times 10^{-6}$ ,  $0.02 \times 10^{-6}$ ,  $0.04 \times 10^{-6}$ ,  $0.06 \times 10^{-6}$ ,  $0.08 \times 10^{-6}$ ,  $0.1 \times 10^{-6}$ , and  $0.125 \times 10^{-6}$  M. c) Normalized emission spectra of PYC12/COONa- $\gamma$ CD, and absorption and emission spectra of EY. d) Fluorescence spectra of PYC12/COONa- $\gamma$ CD (PYC12 =  $20 \times 10^{-6}$  M, COONa- $\gamma$ CD =  $3 \times 10^{-6}$  M) with different concentration of EY. The concentrations of EY were  $0.00 \times 10^{-6}$ ,  $0.01 \times 10^{-6}$ ,  $0.02 \times 10^{-6}$ ,  $0.03 \times 10^{-6}$ ,  $0.04 \times 10^{-6}$ ,  $0.05 \times 10^{-6}$ ,  $0.06 \times 10^{-6}$ , and  $0.08 \times 10^{-6}$  M ( $\lambda_{\text{ex}} = 320$  nm).

Information). In the PYC12/COONa- $\gamma$ CD assembly, the fluorescence lifetimes was  $\tau_1 = 12.49$  ns and  $\tau_2 = 36.94$  ns. However, in the PYC12/COONa- $\gamma$ CD/NiR triad assembly was decreased to  $\tau_1 = 5.04$  ns and  $\tau_2 = 18.8$  ns, and in the PYC12/COONa- $\gamma$ CD/EY triad assembly was decreased to  $\tau_1 = 4.65$  ns and  $\tau_2 = 19.27$  ns compared with PYC12/COONa- $\gamma$ CD assembly (Figures S28 and S29, Supporting Information). In addition, the morphology and size distribution of the PYC12/COONa- $\gamma$ CD/NiR or PYC12/COONa- $\gamma$ CD/EY triad assembly were similar to that of PYC12/COONa- $\gamma$ CD assembly through TEM and DLS experiments, respectively (Figure S30, Supporting Information). Similarly, zeta potential did not change significantly with the addition of energy acceptor (Figure S31, Supporting Information).

Benefiting from the dynamic noncovalent loading, we further constructed multicolor and pure white light-emitting solutions and gels through tuning the molar ratios of donor and acceptor. High FRET efficiency are conducive to the preparation of various monochromatic lights, and moderate FRET efficiency could be used to produce composite lights (for example, white light).<sup>[19]</sup> The CIE chromaticity diagram in Figure 3b,d exhibited the color-tuning maps with adjusting the concentration of acceptor. More importantly, in the PYC12/COONa- $\gamma$ CD/NiR triad assembly, with the addition of NiR to PYC12/COONa- $\gamma$ CD assembly, the emission color changed from cyan to red, which included the white-light emission with the chromaticity coordinates in (0.32, 0.30). Adding EY to PYC12/COONa- $\gamma$ CD assembly changed the emission color from cyan to yellow. As shown in Figure 3, the bright

cyan, white, yellow, and red light-emitting solutions were easily prepared by tuning the energy transfer efficiency. Utilizing the multicolor emission property of light-harvesting supramolecular assembly, multicolor emission hydrogel was prepared through dispersion of agarose gel in the light-harvesting supramolecular assembly. As shown in Figure 3e, four luminescence hydrogels with cyan, white, yellow, and red emission could be observed by the naked eye under excited at 365 nm.

In order to achieve the photoswitchable fluorescence behavior of the present light-harvesting system, we introduced a photoresponsive energy acceptor DAE<sup>[20]</sup> into the PYC12/COONa- $\gamma$ CD/NiR triad light-harvesting assembly. Dithienylethene are recognized as promising photochromic molecule due to their excellent photoisomerization ability between open and closed forms.<sup>[20,21]</sup> The open form of DAE showed an absorption maximum at 301 nm. When irradiated with UV light (254 nm), the absorption peak at 301 nm decreased and simultaneously a new absorption peak appeared at 592 nm, accompanied by an obvious color change of the solution from colorless to blue (Figure S32, Supporting Information). As shown in Figure 4a, the UV-vis spectrum of OF-DAE exhibited poor overlap with the emission of PYC12/COONa- $\gamma$ CD/NiR assembly. However the UV-vis spectrum of CF-DAE gave excellent overlap with the emission of PYC12/COONa- $\gamma$ CD/NiR assembly, which could facilitate the efficient energy transfer process. On the basis of these results, we speculate the photocontrolled light-harvesting system could be achieved. Upon irradiating the DAE-loaded PYC12/COONa- $\gamma$ CD/NiR supramolecular light-harvesting

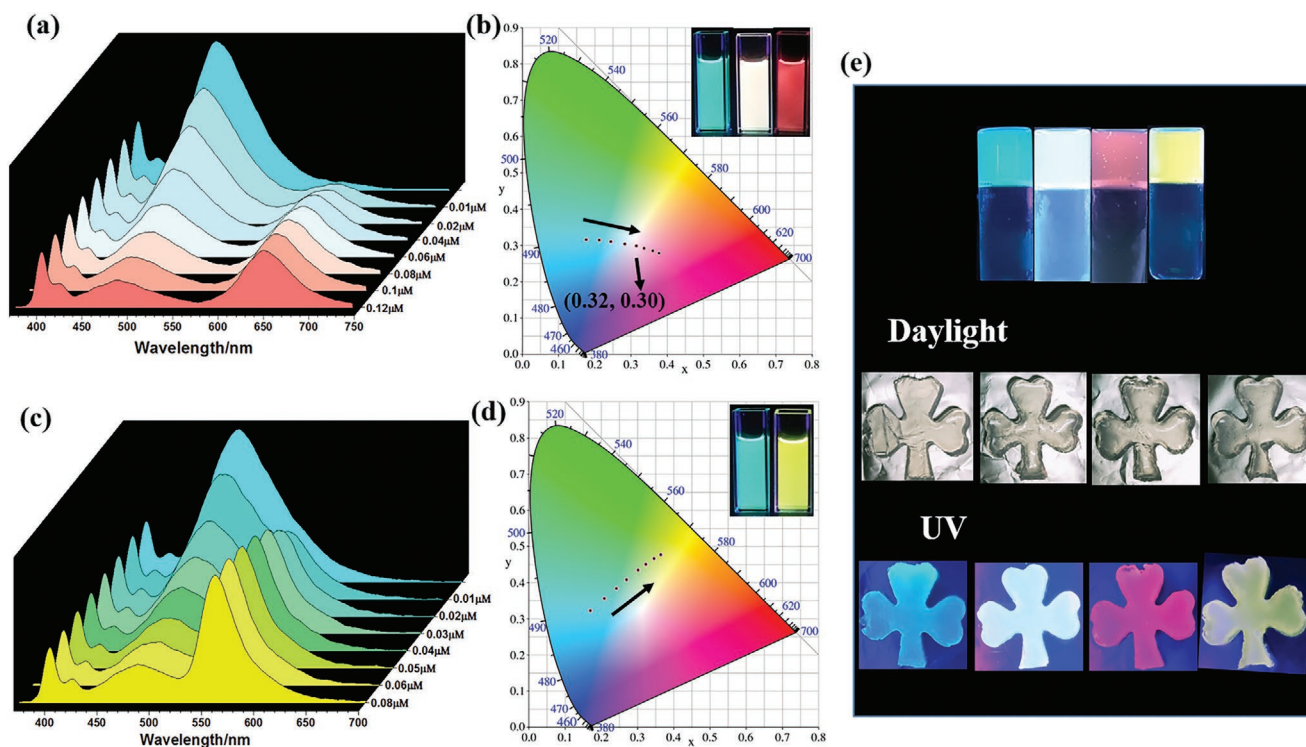


**Figure 3.** a) Fluorescence spectra and b) the CIE chromaticity diagram showing the photoluminescence color changes of PYC12/COONa- $\gamma$ CD with different concentration of NiR. Inset: photographs of PYC12/COONa- $\gamma$ CD and PYC12/COONa- $\gamma$ CD/NiR under 365 nm light. c) Fluorescence spectra and d) the CIE chromaticity diagram showing the photoluminescence color changes of PYC12/COONa- $\gamma$ CD with different concentration of EY. Inset: photographs of PYC12/COONa- $\gamma$ CD and PYC12/COONa- $\gamma$ CD/EY under 365 nm light. e) Photographs of multicolor emission hydrogel under daylight and 365 nm light.

system with UV light, the fluorescence intensity at 640 nm decreased due to the energy transfer from PYC12/COONa- $\gamma$ CD/NiR to CF-DAE (Figure 4b), the energy transfer efficiency was calculated as 76.6%. Subsequently, the fluorescence of the resultant supramolecular assembly was recovered upon >600 nm visible light irradiation arising from the regeneration of OF-DAE (Figure S33, Supporting Information).

In summary, we have successfully constructed photocontrolled artificial light-harvesting system by COONa- $\gamma$ CD-induced excimer emission. The PYC12/COONa- $\gamma$ CD supramolecular assembly was conveniently fabricated via the electrostatic

interaction and hydrophobic interaction in aqueous solution. COONa- $\gamma$ CD could induce the aggregation of PYC12 to generate strong red-shift excimer emission because of the aggregation-induced excimer emission, which made PYC12/COONa- $\gamma$ CD act as antenna donor coassembled with NiR to fabricate efficient artificial light-harvesting materials based on efficient FRET process. And the light-harvesting system exhibited high donor/acceptor ratio, antenna effect and energy transfer efficiency. More importantly, broad-spectrum multicolor photoluminescence including white-light emission was achieved by tuning the energy transfer efficiency. Furthermore,

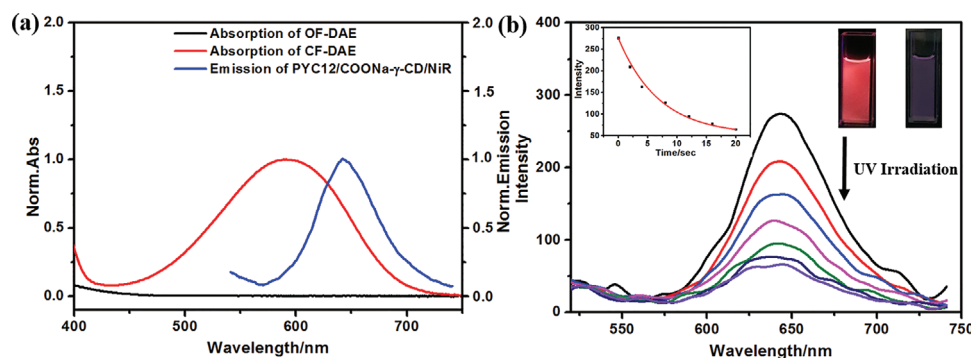


**Figure 4.** a) Normalized absorption spectra of DAE and fluorescence emission of PYC12/COONa- $\gamma$ CD/NiR. b) Fluorescence spectra of PYC12/COONa- $\gamma$ CD/NiR loaded with DAE upon irradiation with UV light (254 nm) ( $\lambda_{\text{ex}} = 320$  nm, PYC12 =  $20 \times 10^{-6}$  M, COONa- $\gamma$ CD =  $3 \times 10^{-6}$  M, NiR =  $0.125 \times 10^{-6}$  M, DAE =  $0.5 \times 10^{-6}$  M).

a photoresponsive energy acceptor DAE was encapsulated into the PYC12/COONa- $\gamma$ CD/NiR light-harvesting system, the fluorescence of the supramolecular nanoparticles could be reversibly switched on/off by irradiation with UV or visible light. Thus, these multicolor tunable luminescent supramolecular light-harvesting systems provided a convenient strategy for mimicking artificial photosynthesis.

## Supporting Information

Supporting Information is available from the Wiley Online Library or from the author.

## Acknowledgements

The authors thank NNSFC (no. 21772100 and 21772099) for the financial support.

## Conflict of Interest

The authors declare no conflict of interest.

## Keywords

aggregation-induced excimer emission, cyclodextrin, light-harvesting systems, photocontrolled, supramolecular assembly

Received: October 3, 2020

Revised: November 3, 2020

Published online: November 23, 2020

- [1] a) G. R. Fleming, G. S. Schlau-Cohen, K. Amarnath, J. Zaks, *Faraday Discuss.* **2012**, *155*, 27; b) G. D. Scholes, G. R. Fleming, A. Olaya-Castro, R. van Grondelle, *Nat. Chem.* **2011**, *3*, 763; c) D. N. Li, W. Li, H. R. Zhang, X. J. Zhang, J. L. Zhuang, Y. L. Liu, C. F. Hu, B. F. Lei, *ACS Appl. Mater. Interfaces* **2020**, *12*, 21009.
- [2] A. Hagfeldt, G. Boschloo, L. Sun, L. Kloo, H. Pettersson, *Chem. Rev.* **2010**, *110*, 6595.
- [3] a) L. K. Ji, Y. T. Sang, G. H. Ouyang, D. Yang, P. F. Duan, Y. Q. Jiang, M. H. Liu, *Angew. Chem., Int. Ed.* **2019**, *58*, 844; b) S. Kuila, S. J. George, *Angew. Chem., Int. Ed.* **2020**, *59*, 9393.
- [4] a) M. Hao, G. P. Sun, M. Z. Zuo, Z. Q. Xu, Y. Chen, X. Y. Hu, L. Y. Wang, *Angew. Chem., Int. Ed.* **2020**, *59*, 10095; b) Z. Y. Zhang, Z. Q. Zhao, Y. L. Hou, H. Wang, X. P. Li, G. He, M. M. Zhang, *Angew. Chem., Int. Ed.* **2019**, *58*, 8862.
- [5] M. Li, S. Long, Y. Kang, L. Guo, J. Wang, J. Fan, J. Du, X. Peng, *J. Am. Chem. Soc.* **2018**, *140*, 15820.
- [6] X. M. Chen, Q. Cao, H. K. Bisoyi, M. Wang, H. Yang, Q. Li, *Angew. Chem., Int. Ed.* **2020**, *59*, 10493.
- [7] N. Melnychuk, S. Egloff, A. Runser, A. Reisch, A. S. Klymchenko, *Angew. Chem., Int. Ed.* **2020**, *59*, 6811.
- [8] a) H. Kashida, H. Azuma, R. Maruyama, Y. Araki, T. Wada, H. Asanuma, *Angew. Chem., Int. Ed.* **2020**, *59*, 11360; b) K. Acharyya, S. Bhattacharyya, H. Sepehrpour, S. Chakraborty, S. Lu, B. Shi, X. Li, P. S. Mukherjee, P. J. Stang, *J. Am. Chem. Soc.* **2019**, *141*, 14565; c) C. Li, J. Zhang, S. Zhang, Y. Zhao, *Angew. Chem., Int. Ed.* **2019**, *58*, 1643; d) Y. Li, Y. Dong, L. Cheng, C. Qin, H. Nian, H. Zhang, Y. Yu, L. Cao, *J. Am. Chem. Soc.* **2019**, *141*, 8412; e) P. Wang, X. Miao, Y. Meng, Q. Wang, J. Wang, H. Duan, Y. Li, C. Li, J. Liu, L. Cao, *ACS Appl. Mater. Interfaces* **2020**, *12*, 22630; f) X. Zhu, J. X. Wang, L. Y. Niu, Q. Z. Yang, *Chem. Mater.* **2019**, *31*, 3573.
- [9] a) H. Q. Peng, L. Y. Niu, Y. Z. Chen, L. Z. Wu, C. H. Tung, Q. Z. Yang, *Chem. Rev.* **2015**, *115*, 7502; b) A. J. P. Teunissen, C. Perez-Medina, A. Meijerink, W. J. M. Mulder, *Chem. Soc. Rev.* **2018**, *47*, 7027; c) L. Wu, C. Huang, B. P. Emery, A. C. Sedgwick, S. D. Bull, X. P. He, H. Tian, J. Yoon, J. L. Sessler, T. D. James, *Chem. Soc. Rev.* **2020**, *49*, 5110.
- [10] a) T. X. Xiao, W. W. Zhong, L. Zhou, L. X. Xua, X. Q. Sun, R. B. P. Elmesb, X. Y. Hu, L. Y. Wang, *Chin. Chem. Lett.* **2019**, *30*, 31; b) H. J. Kim, P. C. Nandajan, J. Gierschner, S. Y. Park, *Adv. Funct. Mater.* **2018**, *28*, 1705141; c) Z. Xu, S. Peng, Y. Y. Wang, J. K. Zhang, A. I. Lazar, D. S. Guo, *Adv. Mater.* **2016**, *28*, 7666; d) D. P. Zhang, Y. N. Liu, Y. J. Fan, C. Y. Yu, Y. L. Zheng, H. B. Jin, L. I. Fu, Y. F. Zhou, D. Y. Yan, *Adv. Funct. Mater.* **2016**, *26*, 7652.
- [11] L. X. Xu, Z. X. Wang, R. R. Wang, L. Y. Wang, X. W. He, H. F. Jiang, H. Tang, D. R. Cao, B. Z. Tang, *Angew. Chem., Int. Ed.* **2019**, *59*, 9908.
- [12] J. Pruchyathamkorn, W. J. Kendrick, A. T. Frawley, A. Mattioni, F. Caycedo-Soler, S. F. Huelga, M. B. Plenio, H. L. Anderson, *Angew. Chem., Int. Ed.* **2020**, *59*, 16455.
- [13] a) S. Guo, Y. Song, Y. He, X. Y. Hu, L. Wang, *Angew. Chem., Int. Ed.* **2018**, *57*, 3163; b) G. Sun, W. Qian, J. Jiao, T. Han, Y. Shi, X. Y. Hu, L. Wang, *J. Mater. Chem. A* **2020**, *8*, 9590; c) T. Xiao, H. Wu, G. Sun, K. Diao, X. Wei, Z. Y. Li, X. Q. Sun, L. Wang, *Chem. Commun.* **2020**, *56*, 12021.
- [14] a) J. J. Li, Y. Chen, J. Yu, N. Cheng, Y. Liu, *Adv. Mater.* **2017**, *29*, 1701905; b) J. J. Li, H. Y. Zhang, X. Y. Dai, Z. X. Liu, Y. Liu, *Chem. Commun.* **2020**, *56*, 5949.
- [15] a) S. H. Li, X. Xu, Y. Zhou, Q. Zhao, Y. Liu, *Org. Lett.* **2017**, *19*, 6650; b) X. L. Ni, S. Chen, Y. Yang, Z. Tao, *J. Am. Chem. Soc.* **2016**, *138*, 6177; c) Q. W. Zhang, D. Li, X. Li, P. B. White, J. Mecinović, X. Ma, H. Ågren, R. J. M. Nolte, H. Tian, *J. Am. Chem. Soc.* **2016**, *138*, 13541; d) X. M. Chen, Y. Chen, Y. Liu, *Chin. J. Chem.* **2018**, *36*, 526; e) J. J. Li, H. Y. Zhang, Y. Zhang, W. L. Zhou, Y. Liu, *Adv. Opt. Mater.* **2019**, *7*, 1900589; f) X.-M. Chen, Y. Chen, Q. Yu, B.-H. Gu, Y. Liu, *Angew. Chem., Int. Ed.* **2018**, *57*, 12519.
- [16] Y. X. Hu, W. J. Li, P. P. Jia, X. Q. Wang, L. Xu, H. B. Yang, *Adv. Opt. Mater.* **2020**, *8*, 2000265.
- [17] Q. Wang, Q. Zhang, Q. W. Zhang, X. Li, C. X. Zhao, T. Y. Xu, D. H. Qu, H. Tian, *Nat. Commun.* **2020**, *11*, 158.
- [18] a) N. Li, L. Qi, J. Qiao, Y. Chen, *Anal. Chem.* **2016**, *88*, 1821; b) G. Singh, P. K. Singh, *Langmuir* **2019**, *35*, 14628.
- [19] W. J. Guan, T. T. Yang, C. Lu, *Angew. Chem., Int. Ed.* **2020**, *59*, 12800.
- [20] G. X. Liu, Y. M. Zhang, C. H. Wang, Y. U. Liu, *Chem. - Eur. J.* **2017**, *23*, 14425.
- [21] a) G. Liu, Y. M. Zhang, L. Zhang, C. Wang, Y. Liu, *ACS Appl. Mater. Interfaces* **2018**, *10*, 12135; b) H. Wu, Y. Chen, X. Dai, P. Li, J. F. Stoddart, Y. Liu, *J. Am. Chem. Soc.* **2019**, *141*, 6583; c) H. Wu, Y. Chen, Y. Liu, *Adv. Mater.* **2017**, *29*, 1605271.